

# Deformed two-dimensional rogue waves in the $(2+1)$ -dimensional Korteweg-de Vries equation

Yulei Cao<sup>1</sup>, Peng-Yan Hu<sup>2\*</sup>, Yi Cheng<sup>3</sup> and Jingsong He<sup>1</sup>

**Abstract.** Within the  $(2+1)$ -dimensional Korteweg-de Vries equation framework, new bilinear Bäcklund transformation and Lax pair are presented based on the binary Bell polynomials and gauge transformation. By introducing an arbitrary function  $\phi(y)$ , a family of deformed soliton and deformed breather solutions are presented with the improved Hirota's bilinear method. Choosing the appropriate parameters, their interesting dynamic behaviors are shown in three-dimensional plots. Furthermore, novel rational solutions are generated by taking the limit of obtained solitons. Additionally, two dimensional [2D] rogue waves (localized in both space and time) on the soliton plane are presented, we refer to it as deformed 2D rogue waves. The obtained deformed 2D rogue waves can be viewed as a 2D analog of the Peregrine soliton on soliton plane, and its evolution process is analyzed in detail. The deformed 2D rogue wave solutions are constructed successfully, which are closely related to the arbitrary function  $\phi(y)$ . This new idea is also applicable to other nonlinear systems.

**Keywords:** 2D KdV equation · Bilinear method · Bäcklund transformation · Lax pair · Deformed 2D rogue wave

**PACS numbers:** 05.45.Yv · 02.30.Jr · 02.30.Ik

## 1. Introduction

Rogue waves (RWs) in the ocean, also known as killer waves, monster waves, freak waves and extreme waves, are special waves with extremely destructive, which should be responsible for some maritime disasters. The main feature of RW is that "appear from nowhere and disappear without a trace"[1]. Peregrine was the first one who obtained the RW solution from one-dimensional systems[2], so such RW solution is also called "Peregrine soliton". These RWs are localized in both space and time in one-dimensional systems[3]-[9], and its dynamic behaviors are similar to that of lumps in high-dimensional systems[10]-[14]. RWs in high-dimensional systems are often called line RWs, which are merely localized in time[15]-[18]. The study of RW has been widely used in diverse areas of theoretical and applied physics, including plasma physics[19, 20], Bose-Einstein condensates[21, 22], atmosphere physics[23], optics and photonics[24, 25, 26] and superfluids[27].

Now, a fundamental problem occurs: Is it possible that other types of RW solutions exist in nonlinear systems? As well as seeking new exact solution for nonlinear systems is an open problem and a challenging work. Furthermore, in integrable system, the Peregrine soliton only appears in the one-dimensional systems. But, the RWs, which are localized in time and space, have never been found in the high-dimensional system. Therefore, searching for the RW solution that is local in time and space of high-dimensional systems has always been an open problem. Until recently, Guo et al.[28] obtained RW solutions, which are localized in both space and time, from a two-dimensional nonlinear Schrödinger model by the even-fold Darboux transformation. Now the long-standing problem of the construction of two-dimensional [2D] rogue wave on zero background is addressed[28]. This is a pioneering work, which

\* Corresponding author: pyhu@szu.edu.cn.

inspires us to explore the structure of 2D RW solutions of other high-dimensional soliton equations. Additionally, RW solutions of complex nonlinear equations have been widely researched, but the RW solutions of real nonlinear equations are rarely mentioned, which is another motivation.

Inspired by the above considerations, in this paper, we focus on the  $(2 + 1)$ -dimensional [2D] Korteweg-de Vries [KdV] equation

$$U_t + U_{xxx} - 3(UV)_x = 0, \quad U_x = V_y, \quad (1)$$

which was first derived by Boiti-Leon-Manna-Pempinelli with a weak Lax pair[29], and can be reduced to the celebrated KdV equation if  $x = y$ . Equation(1) is an asymmetric part of the Nizhnik-Novikov-Veselov [NNV] equation[30], thus equation(1) is also called ANNV equation; this equation(1) can also be derived by using the inner parameter-dependent symmetry constraint of the KP equation[30], and can be considered as a model of an incompressible fluid where  $U$  and  $V$  are the component of velocity[31]. Equation(1) was also regarded to be a generalization[32] of the results of Hirota and Satsuma[33] in the  $(2 + 1)$  dimension.

Letting  $U = W_y, V = W_x$ , then equation(1) reduce to the following single equation,

$$W_{yt} + W_{xxx} - 3W_{xx}W_y - 3W_xW_{xy} = 0. \quad (2)$$

This equation(2) known as BLMF equation was widely investigated. The Cauchy problem, associated with initial data decaying sufficiently rapidly at infinity, was solved by means of inverse scattering transformation[29]. The spectral transformation, nonclassical symmetries and Painlevé property for equation(2) has been researched in Refs.[29, 34, 35]. And a series of Bäcklund transformations[36, 37, 38], Lax pairs[38], supersymmetric[39], soliton-like[40]-[43], breather[44, 45] and lump-type[46, 47, 48] solutions are derived.

In this letter, we are committed to exploring new Bäcklund transformations, Lax pairs and new RW solutions of 2D KdV equation(1) by the Hirota method. The new RW solution is called deformed 2D RW because its formula involves an arbitrary function  $\phi(y)$  which provides a deformed background for rogue wave. This arbitrary function  $\phi(y)$  comes from the crucial bilinear transformation which maps  $U$  to a bilinear form. In section2, new Bäcklund transformations and Lax pair are derived based on the binary Bell polynomials and linearizing the bilinear equation. In section3, we obtain deformed kink soliton and deformed breather solutions of 2D KdV equation by means of the Hirota method. In section4, a family of new rational solutions and deformed 2D RW solutions of the equation(1) are presented by introducing an arbitrary function  $\phi(y)$ . The main results of the paper are summarized and discussed in section5.

## 2. Bilinear Bäcklund transformation and associated Lax pair

In this section, we mainly focus on the new Bäcklund transformation and Lax pair of 2D KdV equation(1). Bäcklund transformation and lax pair are recognized as the main characteristics of integrability, which can be used to obtain exact solutions of nonlinear systems. We first introduce the following variables transformation

$$U = -q_{xy}, \quad V = -q_{xx}, \quad (3)$$

then 2D KdV equation(1) becomes

$$E(q) = q_{yt} + q_{xxx} + 3q_{xx}q_{xy} = 0, \quad (4)$$

two different solutions  $q = 2 \ln G$  and  $\tilde{q} = 2 \ln F$  of equation(1) are introduced, the corresponding two-field condition is as follows[49]-[53]

$$E(\tilde{q}) - E(q) = (\tilde{q} - q)_{yt} + (\tilde{q} - q)_{xxx} + 3(\tilde{q}_{xx}\tilde{q}_{xy} - q_{xx}q_{xy}) = 0. \quad (5)$$

We introduce two new variables

$$v = \frac{\tilde{q} - q}{2} = \ln \frac{F}{G}, \quad w = \frac{\tilde{q} + q}{2} = \ln FG. \quad (6)$$

Based on the binary Bell polynomials, equation(5) can be rewritten into  $\mathcal{Y}$ -polynomials from Bell polynomial theory as follows and rewrite the equation(5) into the form (see Refs. [51, 52, 53] for details)

$$\begin{aligned} E(\tilde{q}) - E(q) &= 2[v_{yt} + v_{xxxy} + 3w_{xx}v_{xy} + 3w_{xy}v_{xx}] \\ &= 2[\partial_y(\mathcal{Y}_{xxx} + \mathcal{Y}_t) + 3w_{xy}v_{xx} - 3w_{xxy}v_x - 3v_x^2v_{xy}]. \end{aligned} \quad (7)$$

Through the following constraints

$$w_{xy} + v_x v_y - \lambda v_x = 0, \quad (8)$$

where  $\lambda$  is the constant parameter. Then, the following coupled system of  $\mathcal{Y}$ -polynomials of equation(1) is deduced

$$\begin{aligned} \mathcal{Y}_{xy} - \lambda \mathcal{Y}_x &= 0, \\ \mathcal{Y}_{xxx} + \mathcal{Y}_t &= 0. \end{aligned} \quad (9)$$

According to the relationship between  $\mathcal{Y}$ -polynomials[51, 52, 53] and bilinear operators  $D$ [54]

$$\mathcal{Y}_{n_1 x_1, \dots, n_l x_l}(v = \ln \frac{F}{G}, w = \ln FG) = (FG)^{-1} D_{x_1}^{n_1} \dots D_{x_l}^{n_l} F \cdot G, \quad (10)$$

the following bilinear Bäcklund transformation is derived for the 2D KdV equation(1)

$$\begin{aligned} (D_x D_y - \lambda D_x) F \cdot G &= 0, \\ (D_x^3 + D_t) F \cdot G &= 0. \end{aligned} \quad (11)$$

Then logarithmic linearization of  $\mathcal{Y}$ -polynomials under the Hopf-Cole transformation  $v = \ln \psi$ , and Bell polynomial formula

$$\begin{aligned} &(FG)^{-1} D_{x_1}^{n_1} \dots D_{x_l}^{n_l} F \cdot G \Big|_{G=e^{\frac{q}{2}}, \frac{F}{G}=\psi} \\ &= \sum_{r_1 + \dots + r_l = \text{even}} \sum_{r_1=0}^{n_1} \dots \sum_{r_l=0}^{n_l} \prod_{i=1}^l \binom{n_i}{r_i} P_{r_1 x_1 \dots r_l x_l}(q) \\ &\quad \times \mathcal{Y}_{(n_1 - r_1) x_1, \dots, (n_l - r_l) x_l}(v), \end{aligned} \quad (12)$$

the  $\mathcal{Y}$ -polynomials can be written as

$$\mathcal{Y}_{n_1 x_1, \dots, n_l x_l}(v) = \frac{\psi_{n_1 x_1, \dots, n_l x_l}}{\psi}, \quad (13)$$

thus the system(9) is then linearized into a Lax pair

$$\begin{aligned} \psi_{xy} + q_{xy} \psi - \lambda \psi_x &= 0, \\ \psi_{xxx} + 3q_{xx} \psi_x + \psi_t &= 0, \end{aligned} \quad (14)$$

which is equivalent to the Lax pair of equation(1)[36]

$$\begin{aligned} \psi_{xy} - U \psi - \lambda \psi_x &= 0, \\ \psi_{xxx} - 3V \psi_x + \psi_t &= 0. \end{aligned} \quad (15)$$

In order to get a new Bäcklund transformation, we introduce the following gauge transformation to the bilinear Bäcklund transformation(11)

$$F \rightarrow e^\xi F, \quad G \rightarrow e^\eta G, \quad (16)$$

where  $\xi = m_1 x + n_1 y + l_1 t$  and  $\eta = m_2 x + n_2 y + l_2 t$ . System(11) is transformed into

$$\begin{aligned} [(D_x + m_1 - m_2)(D_y + n_1 - n_2) - \lambda(D_x + m_1 - m_2)] F \cdot G &= 0, \\ [(D_x + m_1 - m_2)^3 + (D_t + l_1 - l_2)] F \cdot G &= 0, \end{aligned} \quad (17)$$

under the following constraints

$$m_1 - m_2 = \lambda, \quad n_1 - n_2 = \lambda, \quad l_2 - l_1 = \lambda^3. \quad (18)$$

Then, a new Bäcklund transformation of equation(1) is derived as follows

$$\begin{aligned} (D_x D_y + \lambda D_y)F \cdot G &= 0, \\ (D_x^3 + 3\lambda D_x^2 + 3\lambda^2 D_x + D_t)F \cdot G &= 0. \end{aligned} \quad (19)$$

Similarly, the Lax pair of system(25) is as follows

$$\begin{aligned} \psi_{xy} + \lambda\psi_y + q_{xy}\psi &= 0, \\ \psi_{xxx} + 2\lambda\psi_{xx} + 3(\lambda^2 + q_{xx})\psi_x + 3\lambda q_{xx}\psi + \psi_t &= 0, \end{aligned} \quad (20)$$

or equivalently

$$\begin{aligned} (L_1 - U)\psi &= \psi_{xy} + \lambda\psi_y - U\psi = 0, \\ (\partial_t + L_2)\psi &= \psi_{xxx} + 2\lambda\psi_{xx} + 3(\lambda^2 - V)\psi_x - 3\lambda V\psi + \psi_t = 0. \end{aligned} \quad (21)$$

It is easy to check that the integrability condition  $[L_1 - U, \partial_t + L_2]\psi = 0$  is satisfied.

Additionally, another form of Bäcklund transformation and lax pair of 2D KdV equation(1) are also derived, when taking

$$U = -2\partial_{xy} \ln f(x, y, t) + \phi(y), \quad V = -2\partial_{xx} \ln f(x, y, t), \quad (22)$$

2D KdV equation(1) is then translated into the following bilinear form,

$$[D_x^3 D_y + D_y D_t - 3\phi(y)D_x^2]f(x, y, t) \cdot f(x, y, t) = 0, \quad (23)$$

$\phi(y)$  is an arbitrary function of  $y$ ,  $f$  is a real function and  $D$  is the Hirota's bilinear differential operator[54], based on the binary Bell polynomials[49, 50, 51], equation(1) admits the following Bäcklund transformation

$$\begin{aligned} [D_x D_y - \phi(y)]F \cdot G &= 0, \\ [D_x^3 + D_t + k]F \cdot G &= 0. \end{aligned} \quad (24)$$

If using gauge transformation(16) to the above bilinear Bäcklund transformation(24), a new Bäcklund transformation of equation(1) is derived

$$\begin{aligned} [D_x D_y + \lambda(D_x + D_y) + \lambda^2 - \phi(y)]F \cdot G &= 0, \\ [D_x^3 + 3\lambda D_x^2 + 3\lambda^2 D_x + D_t + k]F \cdot G &= 0. \end{aligned} \quad (25)$$

Then, we derive the corresponding linear system under the Hopf-Cole transformation(13)

$$\begin{aligned} \psi_{xy} + \lambda(\psi_x + \psi_y) + (\lambda^2 + q_{xy} - \phi(y))\psi &= 0, \\ \psi_{xxx} + 3\lambda\psi_{xx} + 3(\lambda^2 + q_{xx})\psi_x + \psi_t + (3\lambda q_{xx} + k)\psi &= 0, \end{aligned} \quad (26)$$

which is equivalent to the Lax system of 2D KdV equation(1)

$$\begin{aligned} \psi_{xy} + \lambda(\psi_x + \psi_y) + (\lambda^2 - U)\psi &= 0, \\ \psi_{xxx} + 3\lambda\psi_{xx} + 3(\lambda^2 - V)\psi_x + \psi_t + (k - 3\lambda V)\psi &= 0. \end{aligned} \quad (27)$$

### 3. Deformed multi-kink soliton and deformed breather solutions of the 2D KdV equation

Based on the above new bilinear equation(23), some exact solutions of 2D KdV equation(1), including deformed multi-solitons and deformed breathers, are generated. First, deformed one-soliton solutions take the forms

$$U_{[1]} = -2\partial_{xy} \ln(1 + e^{\eta_1}) + \phi(y), \quad V_{[1]} = -2\partial_{xx} \ln(1 + e^{\eta_1}), \quad (28)$$

where  $\eta_1 = p_1 x + \Phi(y)q_1 y + \Omega_1 t + \eta_1^0$ ,  $\eta_1^0 = 0$  and  $\phi(y) = \frac{d\Phi(y)}{dy}$ . Substituting (28) into (1), the following dispersion relation of 2D KdV equation is obtained

$$\Omega_1 = -\frac{p_1^2(p_1 q_1 - 3)}{q_1}.$$

The exact expression of  $U_{[1]}$  and  $V_{[1]}$  are as follows

$$U_{[1]} = \phi(y) \frac{1 + \cosh\left(p_1 x + q_1 \Phi(y) + \left(\frac{3p_1^2}{q_1} - p_1^3\right)t\right) - p_1 q_1}{1 + \cosh\left(p_1 x + q_1 \Phi(y) + \left(\frac{3p_1^2}{q_1} - p_1^3\right)t\right)},$$

$$V_{[1]} = -\frac{p_1^2}{1 + \cosh\left(p_1 x + q_1 \Phi(y) + \left(\frac{3p_1^2}{q_1} - p_1^3\right)t\right)}.$$
(29)

As can be seen from the above expression, the extremum lines  $p_1 x + q_1 \Phi(y) + \left(\frac{3p_1^2}{q_1} - p_1^3\right)t$  and velocity  $\frac{3p_1 - q_1 p_1^2}{q_1}$  of  $U_{[1]}$  and  $V_{[1]}$  are the same, and the corresponding amplitudes of  $U_{[1]}$  and  $V_{[1]}$  in  $(x, y)$ -plane are  $\phi(y)(1 - \frac{p_1 q_1}{2})$  and  $\frac{p_1^2}{2}$  respectively. Thus,  $U_{[1]}$  is a deformed bright soliton when  $\phi(y)(2 - p_1 q_1) > 0$  and a deformed dark soliton when  $\phi(y)(2 - p_1 q_1) < 0$ . However,  $V_{[1]}$  is always a deformed dark soliton see Fig.1.

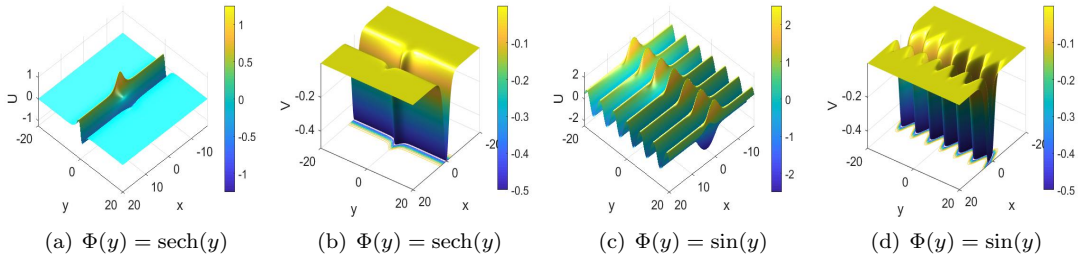


FIGURE 1. Deformed one-soliton  $U_{[1]}$  and  $V_{[1]}$  of equation(1) in the  $(x, y)$ -plane with parameters  $p_1 = 1, q_1 = -4$  and displayed at  $t = 0$ .

In order to obtain deformed two-solitons of 2D KdV equation(1), taking

$$U_{[2]} = -2\partial_{xy} \ln(1 + e^{\eta_1} + e^{\eta_2} + e^{\eta_1 + \eta_2 + A_{12}}) + \phi(y),$$

$$V_{[2]} = -2\partial_{xx} \ln(1 + e^{\eta_1} + e^{\eta_2} + e^{\eta_1 + \eta_2 + A_{12}}),$$
(30)

where  $\eta_1 = p_1 x + \Phi(y)q_1 y + \Omega_1 t + \eta_1^0$  and  $\eta_2 = p_2 x + \Phi(y)q_2 y + \Omega_2 t + \eta_2^0$ . Substituting (30) into (1), the following relations are obtained

$$\Omega_1 = -\frac{p_1^2(p_1 q_1 - 3)}{q_1}, \quad \Omega_2 = -\frac{p_2^2(p_2 q_2 - 3)}{q_2},$$

$$\exp(A_{12}) = \frac{(p_1 q_2 - p_2 q_1)^2 + p_1 p_2 q_1 q_2 (p_1 - p_2)(q_1 - q_2)}{(p_1 q_2 - p_2 q_1)^2 + p_1 p_2 q_1 q_2 (p_1 + p_2)(q_1 + q_2)}.$$
(31)

Further, taking  $p_1 = 3, q_1 = 3, p_2 = \frac{5}{2}, q_2 = 3, \eta_1^0 = -\eta_2^0 = \frac{\pi}{2}$ , the analytical expressions  $U_{[2]}$  and  $V_{[2]}$  of deformed two-soliton solutions are as follows

$$U_{[2]} = \frac{\left\{ \cosh(2\kappa_{11}) - \sinh(2\kappa_{11}) + 982081 \left( \sum_{j=2}^4 [\cosh(2\kappa_{1j}) + \sinh(2\kappa_{1j})] \right) + \left( \sum_{m=1}^5 \Gamma_m [\cosh(\kappa_m) - (-1)^m \sinh(\kappa_m)] \right) \right\}}{\frac{1}{\phi(y)} \left( \cosh(\kappa_{11}) - \sinh(\kappa_{11}) + 991 \sum_{j=2}^4 [\cosh(\kappa_{1j}) + \sinh(\kappa_{1j})] \right)^2}, \quad (32)$$

$$V_{[2]} = \frac{\left\{ [\cosh(3\Phi(y)) + \sinh(3\Phi(y))] \left( \sum_{m=1}^5 \gamma_m [\cosh(\kappa_m - 3(-1)^{m+1}\Phi(y))] \right) - \sum_{m=1}^5 (-1)^m [\sinh(\kappa_m - 3(-1)^{m+1}\Phi(y))] \right\}}{-1982 \left( \frac{1}{991} [\cosh(\kappa_{11}) - \sinh(\kappa_{11})] + \sum_{j=2}^4 [\cosh(\kappa_{1j}) + \sinh(\kappa_{1j})] \right)^2},$$

where

$$\begin{aligned} \kappa_{11} &= -\frac{11}{2}x - 6\Phi(y) + \frac{75}{8}t - \frac{\pi}{2}, & \kappa_{12} &= \frac{5}{2}x + 3\Phi(y) + \frac{69}{8}t, & \kappa_{13} &= 18t + \frac{\pi}{2}, & \kappa_{14} &= 3x + 3\Phi(y), \\ \kappa_1 &= \kappa_{12} + \kappa_{14}, & \kappa_2 &= \kappa_{11} - \kappa_{12}, & \kappa_3 &= \kappa_{12} + \kappa_{13}, & \kappa_4 &= \kappa_{11} - \kappa_{14}, & \kappa_5 &= \kappa_{13} + \kappa_{14}, & \Gamma_1 &= 1900738, \\ \Gamma_2 &= -15856, & \Gamma_3 &= -12767053, & \Gamma_4 &= -12883, & \Gamma_5 &= 15713296, & \gamma_1 &= 1112, & \gamma_2 &= 36, \\ \gamma_3 &= 24775, & \gamma_4 &= 25, & \gamma_5 &= 35676. \end{aligned} \quad (33)$$

The dynamic behaviors of deformed two-soliton solutions are more complex and interesting by choosing the appropriate parameter  $\phi(y)$  see Fig.2. Furthermore, as can be seen the two-dimensional plots of Fig.2, the interaction of deformed two-soliton solutions is an elastic collision.

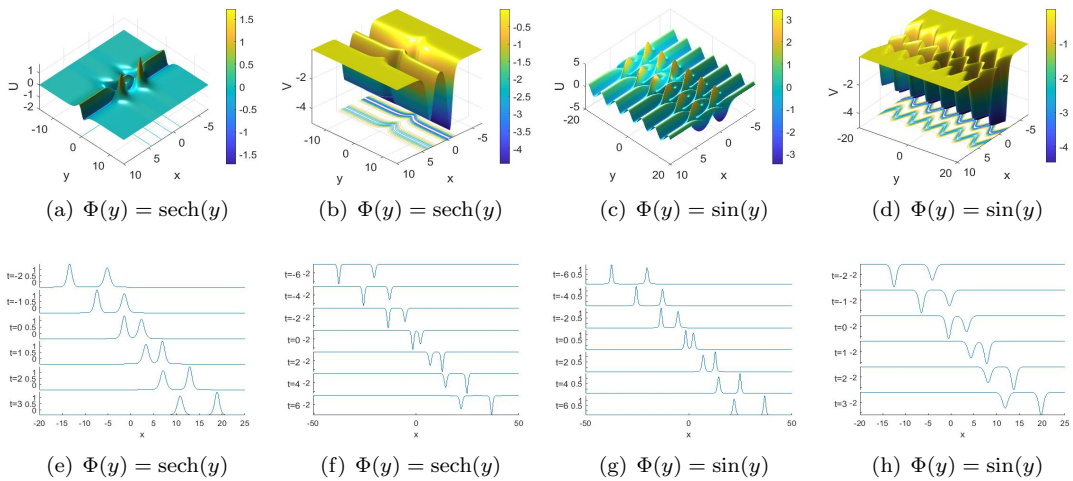


FIGURE 2. Deformed two-soliton solutions  $U_{[2]}$  and  $V_{[2]}$  of equation(1) in the  $(x, y)$ -plane displayed at  $t = 0$ . Panels (a),(b),(c),(d) are the two-dimensional plots of (e),(f),(g),(h) respectively

Similarly,  $N$ -soliton solutions  $U_{[N]}$  and  $V_{[N]}$  are given in equation(22) of the 2D KdV equation(1), in which  $f$  can be written as follows:

$$f = f_{[N]} = \sum_{\mu=0,1} \exp\left(\sum_{j < k}^{(N)} \mu_j \mu_k A_{jk} + \sum_{j=1}^N \mu_j \eta_j\right), \quad (34)$$

here

$$\begin{aligned} \eta_j &= p_j x + \Phi(y) q_j y + \Omega_j t + \eta_j^0, \quad \Omega_j = -\frac{p_j^2(p_j q_j - 3)}{q_j}, \\ \exp(A_{jk}) &= \frac{(p_j q_k - p_k q_j)^2 + p_j p_k q_j q_k (p_j - p_k)(q_j - q_k)}{(p_j q_k - p_k q_j)^2 + p_j p_k q_j q_k (p_j + p_k)(q_j + q_k)}, \end{aligned} \quad (35)$$

where  $p_j, q_j$  are arbitrary real parameters,  $\eta_j^0$  is a complex constant,  $\phi(y)$  is an arbitrary function of  $y$ , and the subscript  $j$  denotes an integer. For higher order soliton solutions, more deformed solitons will be generated from equation(34) with appropriate parameter  $\phi(y)$ , and its dynamic behavior will be more complex, we did not discuss it here.

#### 4. Deformed 2D RW of the 2D KdV equation

In order to obtain the deformed 2D RW solutions of the 2D KdV equation(1), taking

$$q_1 = \lambda_1 p_1, \quad q_2 = \lambda_2 p_2, \quad \eta_1^0 = \eta_2^0 = i\pi, \quad (36)$$

in equation(30) and take a suitable limit as  $p_1, p_2 \rightarrow 0$ , then we further take  $\lambda_1 = a + bi, \lambda_2 = a - bi$  in (36). The solutions  $U^{[1]}$  and  $V^{[1]}$  are given as follows

$$\begin{aligned} U^{[1]}(x, y, t) &= \phi(y) + 4b^2 \phi(y) \frac{ab^2(a^2 + b^2)A_{21}^2 - \frac{b^4}{a}A_{22}^2 - A_{23}}{(A_{11}^2 + A_{12}^2 + A_{13})^2}, \\ V^{[1]}(x, y, t) &= 4b^2 \frac{b^2(a^2 - b^2)(a^2 + b^2)^2 B_{11}^2 - \frac{b^4}{a^2 - b^2} B_{12}^2 - B_{13}}{(A_{11}^2 + A_{12}^2 + A_{13})^2}, \end{aligned} \quad (37)$$

with

$$\begin{aligned} A_{11} &= \frac{3b(a^2 - b^2)}{a^2 + b^2}t + abx + b(a^2 + b^2)\Phi(y), \quad A_{12} = b^2x + \frac{6ab^2}{a^2 + b^2}t, \\ A_{13} &= a(a^2 + b^2)^2, \quad A_{21} = \frac{a^2 + b^2}{a}x + (a^2 + b^2)\Phi(y) + 3t, \\ A_{22} &= 6at + (a^2 + b^2)x, \quad A_{23} = a^2(a^2 + b^2)^3, \quad B_{11} = \frac{a}{a^2 - b^2}x + \Phi(y) + \frac{3}{a^2 - b^2}t, \\ B_{12} &= 6at + (a^2 + b^2)x, \quad B_{13} = a(a^2 + b^2)^3. \end{aligned} \quad (38)$$

As can be seen from the above expression, for ensure that the above solutions  $U^{[1]}$  and  $V^{[1]}$  are smooth, parameter  $a > 0$  must be held.

##### 4.1. Fundamental rational solutions

The fundamental rational solutions  $U^{[1]}$  and  $V^{[1]}$  of 2D KdV equation(1) are derived if  $\phi(y)$  is a polynomial function. Without loss of generality, take  $\phi(y) = 2y$ . The trajectories of  $U^{[1]}$  and  $V^{[1]}$  are as follows

$$\begin{aligned} l_1 &= ax + (a^2 + b^2)y^2 + \frac{3(a^2 - b^2)}{a^2 + b^2}t, \\ l_2 &= x + \frac{6a}{a^2 + b^2}t. \end{aligned} \quad (39)$$

$\lim_{(x,y) \rightarrow \infty} U^{[1]} = 2y$  and  $\lim_{(x,y) \rightarrow \infty} V^{[1]} = 0$ , which show that the background planes of  $U^{[1]}$  and  $V^{[1]}$  are  $2y$  and  $0$ , respectively. Further, taking  $a = 2$  and  $b = 2$ , the exact expression of fundamental rational solutions  $U^{[1]}$  and  $V^{[1]}$  can be obtained. In order to describe the evolution process of fundamental

rational solutions  $U^{[1]}$  more clearly, we removed the background plane  $2y$  when plotting. As shown in Fig.3. the rational solution  $U^{[1]}$  removing the background plane  $2y$  appears from a constant plane when  $t \ll 0$ . With time evolution an arc line  $x = -4y^2$  appears on the constant background around at  $t = 0$  [see the Fig.3(a)], and finally the arc line fission into a bright lump and a dark lump [see the Fig.3(c)]. The trajectories of fission are  $x + 4y^2 = 0$  and  $2x + 3t = 0$  [see the Fig.3(d)(e)].

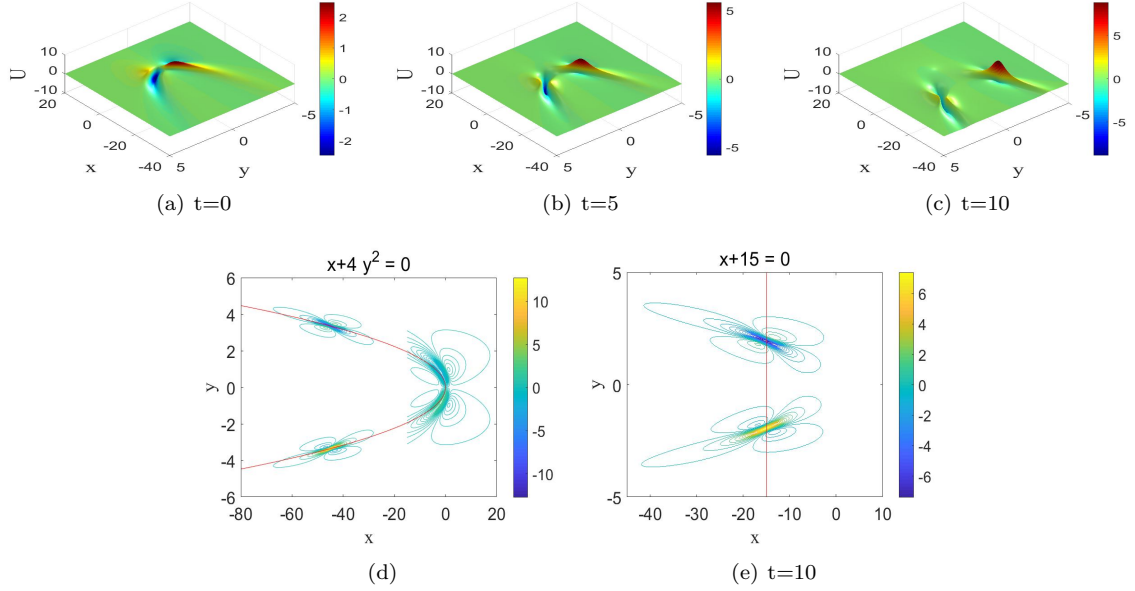


FIGURE 3. The temporal evolution of fundamental rational solution  $U_{[1]}$  removing the background plane  $\phi(y)$  of the equation(1) in the  $(x, y)$ -plane with parameters  $\phi(y) = 2y, a = 2$  and  $b = 2$ ; Panels (d) and (e) are two-dimensional plots of  $U_{[1]}$ .

However, the dynamic behavior of the rational solution  $V^{[1]}$  is different from  $U^{[1]}$ . For given  $\phi(y) = 2y$ , the solution  $V^{[1]}$  has the following nine critical points in  $(x, y)$ -plane

$$\begin{aligned}
 \Lambda_1 &= (x_1, y_1) = \left( \frac{3at}{a^2 + b^2}, y = 0 \right); \\
 \Lambda_{2,3} &= (x_{2,3}, y_{2,3}) = \left( \frac{-3abt \pm \sqrt{3a(a^2 + b^2)^3 + 27b^4t^2}}{b(a^2 + b^2)}, y = 0 \right); \\
 \Lambda_{4,5} &= (x_{4,5}, y_{4,5}) = \left( -\frac{6at}{a^2 + b^2}, y = \pm \sqrt{\frac{3t}{a^2 + b^2}} \right); \\
 \Lambda_{6,7,8,9} &= (x_{6,7,8,9}, y_{6,7,8,9}) = \left( \frac{-6abt \pm \sqrt{3a(a^2 + b^2)^3}}{b(a^2 + b^2)}, y = \pm \sqrt{\frac{3t}{a^2 + b^2}} \right),
 \end{aligned} \tag{40}$$

letting

$$\Delta(x, y) = \frac{\partial^2 V^{[1]}}{\partial x^2}; \quad \mathbf{H}(x, y) = \frac{\partial^2 V^{[1]}}{\partial x^2} \frac{\partial^2 V^{[1]}}{\partial y^2} - \left( \frac{\partial^2 V^{[1]}}{\partial x \partial y} \right)^2, \tag{41}$$



yield

$$\begin{aligned}
 \Delta(x, y) \Big|_{\Lambda_1} &= \frac{24b^4(a^2 + b^2)^4}{[a(a^2 + b^2)^3 + 9b^4t^2]^2}; & \mathbf{H}(x, y) \Big|_{\Lambda_1} &= -\frac{1152b^{10}(a^2 + b^2)^7t}{[a(a^2 + b^2)^3 + 9b^4t^2]^4}, \\
 \Delta(x, y) \Big|_{\Lambda_{2,3}} &= -\frac{3b^4(a^2 + b^2)^4}{4[a(a^2 + b^2)^3 + 9b^4t^2]^2}; & \mathbf{H}(x, y) \Big|_{\Lambda_{2,3}} &= -\frac{9b^{10}(a^2 + b^2)^7t}{2[a(a^2 + b^2)^3 + 9b^4t^2]^4}, \\
 \Delta(x, y) \Big|_{\Lambda_{4,5}} &= \frac{24b^4}{a^2(a^2 + b^2)^2}; & \mathbf{H}(x, y) \Big|_{\Lambda_{4,5}} &= \frac{2304b^10t}{a^4(a^2 + b^2)^5}, \\
 \Delta(x, y) \Big|_{\Lambda_{6,7,8,9}} &= -\frac{3b^4}{4a^2(a^2 + b^2)^2}; & \mathbf{H}(x, y) \Big|_{\Lambda_{6,7,8,9}} &= \frac{9b^{10}t}{a^4(a^2 + b^2)^5}.
 \end{aligned} \tag{42}$$

Based on the above analysis, the evolution of rational solution  $V^{[1]}$  of 2D KdV equation(1) can be divided into the following three stages.

- (i) When  $t < 0$ ,  $\lim_{(x,y) \rightarrow \infty} V^{[1]} = 0$ , which show that rational solution  $V^{[1]}$  appears from a constant background. Now the maximum value  $V_{max}^{[1]}(x, y)$  and minimum value  $V_{min}^{[1]}(x, y)$  of  $V^{[1]}$  are obtained at  $\Lambda_{2,3}$  and  $\Lambda_1$

$$\begin{aligned}
 V_{max}^{[1]}(x, y) = V^{[1]}(x, y) \Big|_{\Lambda_{2,3}} &= \frac{b^2(a^2 + b^2)^2}{2a(a^2 + b^2)^3 + 18b^4t^2}, \\
 V_{min}^{[1]}(x, y) = V^{[1]}(x, y) \Big|_{\Lambda_1} &= -\frac{4b^2(a^2 + b^2)^2}{a(a^2 + b^2)^3 + 9b^4t^2}.
 \end{aligned} \tag{43}$$

Obviously, the global extreme values of rational solution  $V^{[1]}$  changes with time, and

$$\lim_{t \rightarrow -\infty} V_{max}^{[1]}(x, y) = \lim_{t \rightarrow -\infty} V_{min}^{[1]}(x, y).$$

- (ii) When  $t = 0$ , rational solution  $V^{[1]}$  has three extreme points

$$A_1(x, y) = (0, 0), \quad A_2(x, y) = \left(\frac{\sqrt{3a^2 + 3ab^2}}{b}, 0\right), \quad A_3(x, y) = \left(-\frac{\sqrt{3a^2 + 3ab^2}}{b}, 0\right).$$

Maximum and minimum values are as follows

$$\begin{aligned}
 V_{max}^{[1]}(x, y) = V^{[1]}(x, y) \Big|_{A_2} &= V^{[1]}(x, y) \Big|_{A_3} = \frac{b^2}{2a(a^2 + b^2)}, \\
 V_{min}^{[1]}(x, y) = V^{[1]}(x, y) \Big|_{A_1} &= -\frac{4b^2}{a(a^2 + b^2)}.
 \end{aligned} \tag{44}$$

From the above analysis, we can see that its dynamic behavior is similar to the RW in one-dimensional systems. The amplitude of the RW in one-dimensional systems is three times that of the background plane. However, the amplitude of RW of 2D KdV equation(1) is controlled by parameters  $a$  and  $b$ .

- (iii) When  $t > 0$ , rational solution  $V^{[1]}$  has six extreme points  $\Lambda_{4,5}$  and  $\Lambda_{6,7,8,9}$ . And it has four maximums and two minimums

$$\begin{aligned}
 V_{max}^{[1]}(x, y) = V^{[1]}(x, y) \Big|_{\Lambda_{6,7,8,9}} &= \frac{b^2}{2a(a^2 + b^2)}, \\
 V_{min}^{[1]}(x, y) = V^{[1]}(x, y) \Big|_{\Lambda_{4,5}} &= -\frac{4b^2}{a(a^2 + b^2)}.
 \end{aligned} \tag{45}$$

Obviously, the extreme values of  $V^{[1]}$  at  $t = 0$  is equal to the extreme values at  $t > 0$ .

Through the above analysis,  $|V_{max}^{[1]}(x, y)| < |V_{min}^{[1]}(x, y)|$  always satisfied, which indicated that  $V^{[1]}$  is dark. When  $t < 0$ , we know that the rational solution  $V^{[1]}$  appears from a constant plane, and the amplitude above the background plane is 8 times of that below the background plane.  $V^{[1]}$  reaches the maximum amplitude  $\frac{9b^2}{2a(a^2+b^2)}$  at  $t = 0$ . With the time involution, dark lump fission into two identical dark lumps along the curve  $ax + (a^2 + b^2)y^2 + \frac{3(a^2-b^2)}{a^2+b^2}t$ . Interestingly, after the dark lump fission into two identical lumps, its amplitude does not change, which means the energy does not change when  $t > 0$  [see the Fig.4].

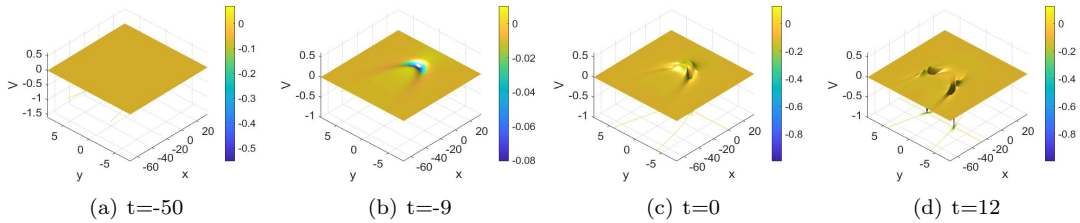


FIGURE 4. The temporal evolution of fundamental rational solution  $V^{[1]}$  of the equation(1) in the  $(x, y)$ -plane with parameters  $\phi(y) = 2y, a = 2$  and  $b = 2$ .

#### 4.2. Fundamental deformed 2D RW solutions

The fundamental deformed 2D RW  $U^{[1]}$  and  $V^{[1]}$  of 2D KdV equation(1) are obtained when  $\phi(y) = \text{sech}(y)$ .  $\lim_{(x,y) \rightarrow \infty} U^{[1]} = \phi(y)$ , which indicated that the background plane of deformed 2D RW  $U^{[1]}$  is  $\phi(y)$ . The trajectories of  $U^{[1]}$  are

$$\begin{aligned} l'_1 &= ax + (a^2 - b^2) \text{sech}(y) + 3t, \\ l'_2 &= x + 2a \text{sech}(y). \end{aligned} \quad (46)$$

As can be seen in Fig.5, in order to better observe the evolution of the deformed 2D RW  $U^{[1]}$ , we remove the background plane of  $U^{[1]}$ . Four panels describe the appearance and annihilation of 2D RW in  $(x, y)$ -plane along the curve  $x + 2 \text{sech}(y)$ . This is the first time to obtain such deformed 2D RW in high-dimensional systems. The dynamic behavior of fundamental deformed 2D RW  $V^{[1]}$  is more complicated and interesting. Through simple calculation and analysis, the evolution of deformed 2D RW  $V^{[1]}$  can be divided into the following four stages

- (i) When  $t < 0$ , a line RW appears from constant background plane, with the time involution, the amplitude of the line RW gradually increases.
- (ii) When  $t = 0$ , the amplitude of the line RW reaches its maximum value. The maximum amplitude  $V_{Amp}^{[1]}$  is

$$V_{Amp}^{[1]} = V_{Max}^{[1]} - V_{Min}^{[1]} = \frac{b^2}{2a(a^2 + b^2)} - \frac{-4b^2}{a(a^2 + b^2)} = \frac{9b^2}{2a(a^2 + b^2)}. \quad (47)$$

- (iii) When  $0 < t \leq \frac{a^2+b^2}{3}$ , the line RW disappears gradually. Simultaneously, a Peregrine-type soliton is generated, but the amplitude of the RW  $V^{[1]}$  is fixed in this process of evolution

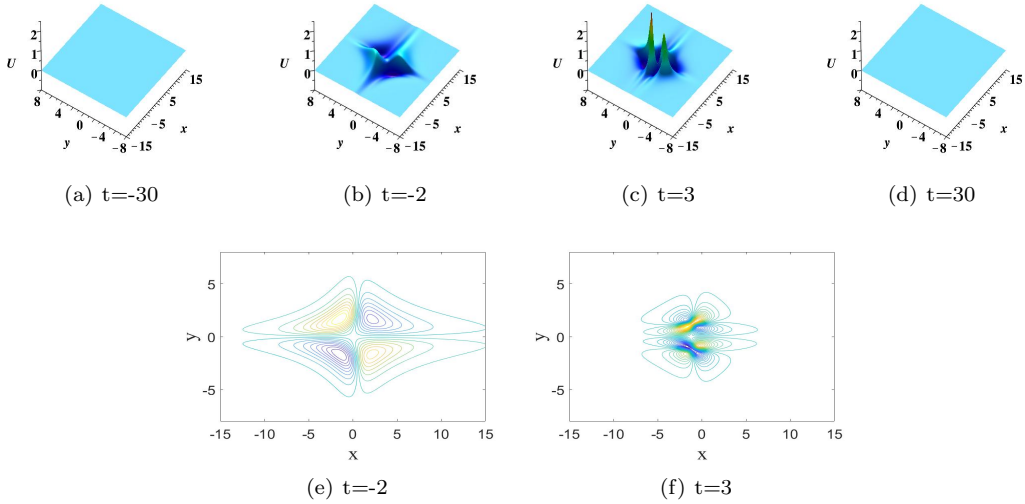


FIGURE 5. The temporal evolution of fundamental deformed 2D RW solution  $U^{[1]}$  removing the background plane  $\phi(y)$  of the equation(1) in the  $(x, y)$ -plane with parameters  $\Phi(y) = \text{sech}(y)$ ,  $a = 1$  and  $b = 4$ .

- (iv) When  $t > \frac{a^2+b^2}{3}$ , two identical maximum values  $V_{Max}^{[1]}$  and one minimum value  $V_{Min}^{[1]}$  of the Peregrine-type soliton are as follows

$$\begin{aligned} V_{Max}^{[1]} &= \frac{b^2(a^2 + b^2)^2}{2b^4(3t - a^2 - b^2)^2 + 2a(a^2 + b^2)^3}, \\ V_{Min}^{[1]} &= -\frac{4b^2(a^2 + b^2)^2}{b^4(3t - a^2 - b^2)^2 + a(a^2 + b^2)^3}. \end{aligned} \quad (48)$$

It can be seen from the above expression that the amplitude of the Peregrine-type soliton decays rapidly in a very short time. When  $t \gg \frac{a^2+b^2}{3}$ , RW  $V^{[1]}$  uniformly approaches a constant background see Fig.6.

### 4.3. High-order deformed 2D RW solutions

When taking

$$N = 4, \quad q_j = \lambda_j p_j, \quad \eta_j^0 = i\pi (j = 1, 2, 3, 4), \quad (49)$$

in equation(34). Further taking

$$\lambda_1 = \lambda_2^* = 1 + 3i, \quad \lambda_3 = \lambda_4^* = \frac{1}{2} - 4i, \quad \Phi(y) = \text{sech}(y), \quad (50)$$

the second-order deformed 2D RW solutions  $U^{[2]} = -2 \ln f_{xy}^{[2]} + \phi(y)$  and  $V^{[2]} = -2 \ln f_{xx}^{[2]}$  are generated, in which  $f^{[2]}$  can be written as,

$$\begin{aligned} f^{[2]}(x, y, t) &= x^4 + [6\Phi(y) + \frac{27}{10}t]x^3 + [21\Phi(y)^2 + \frac{21}{5}\Phi(y)t + \frac{189}{40}t^2 + \frac{149877}{1156}]x^2 + [36\Phi(y)^3 + \frac{27}{10}t\Phi(y)^2 \\ &+ \frac{81}{20}t^2\Phi(y) + \frac{81}{20}t^3 + \frac{2924139}{11560}t]x + \frac{81}{40}t^4 - \frac{81}{20}\Phi(y)t^3 + [\frac{801}{40}\Phi(y)^2 + \frac{688257}{46240}]t^2 + [-\frac{144}{5}\Phi(y)^3 \\ &+ \frac{1008648}{1445}\Phi(y)]t + 40\Phi(y)^4 - \frac{122850}{289}\Phi(y)^2 + \frac{1158885}{89}. \end{aligned} \quad (51)$$

As can be seen in Fig.7, remove the background plane  $\phi(y)$ , the second-order deformed 2D RW solution  $U^{[2]}$  describes that four Peregrine-type solitons appear and annihilate from the constant background

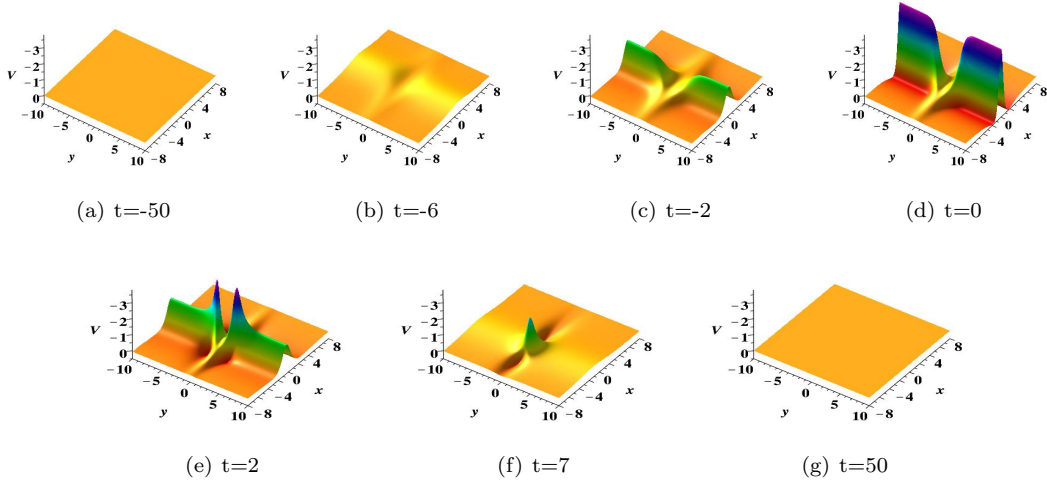


FIGURE 6. The temporal evolution of fundamental deformed 2D RW solution  $V^{[1]}$  of the equation(1) in the  $(x, y)$ -plane with parameters  $\Phi(y) = \text{sech}(y)$ ,  $a = 1$  and  $b = 4$ .

plane. However, the dynamic behaviors of the second-order RW solution  $V^{[2]}$  are similar to that of the fundamental RW solution  $V^{[1]}$ . The RW solution  $V^{[2]}$  is uniformly approach to a constant background plane when  $t \rightarrow \pm\infty$ . Two line RWs appear from the constant plane under the time evolution, and their amplitudes increased rapidly. Then the amplitude of the two line RW attenuated rapidly, at the same time, two Peregrine-type solitons are produced. Finally, these two Peregrine-type solitons disappeared in a very short time without a trace see Fig.8.

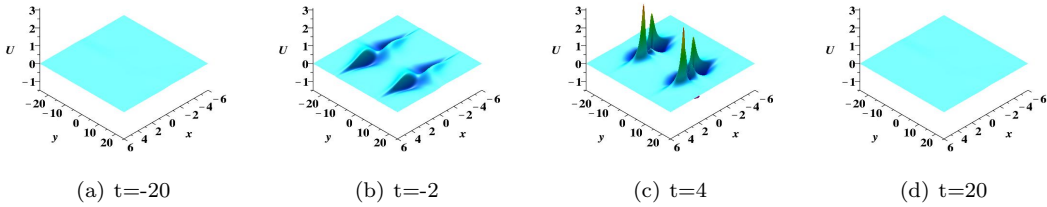


FIGURE 7. The temporal evolution of second-order deformed 2D RW solution  $U^{[2]}$  removing the background plane  $\phi(y)$  of equation(1) in the  $(x, y)$ -plane.

For larger  $N$ , higher-order solutions are generated, taking the parameters

$$N = 2n, \quad q_j = \lambda_j p_j, \quad \eta_j^0 = i\pi \quad (1 \leq j \leq N), \quad (52)$$

in equation(34) and take a suitable long wave limit as  $p_j \rightarrow 0$ , the functions  $f$  defined in (34) become a polynomial-type function containing an arbitrary function  $\phi(y)$ . Therefore, the general  $n$ -th rational-type functions  $U^{[n]} = -2 \ln f_{xy} + \phi(y)$  and  $V^{[n]} = -2 \ln f_{xx}$  of 2D KdV equation(1) can be derived[55], in which  $f$  can be written as follows,

$$f = f^{[n]} = \prod_{k=1}^N \theta_k + \frac{1}{2} \sum_{k,j}^{(N)} \alpha_{kj} \prod_{l \neq k,j} \theta_l + \dots + \frac{1}{M!2^M} \sum_{i,j,\dots,m,n}^{(N)} \overbrace{\alpha_{kj} \alpha_{kl} \dots \alpha_{mn}}^M \prod_{p \neq k,j,\dots,m,n} \theta_p + \dots, \quad (53)$$

with

$$\theta_j = \frac{\lambda_j^2 \phi(y) + \lambda_j x + 3t}{\lambda_j}, \quad \alpha_{jk} = -\frac{2\lambda_j \lambda_k (\lambda_j + \lambda_k)}{(\lambda_j - \lambda_k)^2}, \quad (54)$$

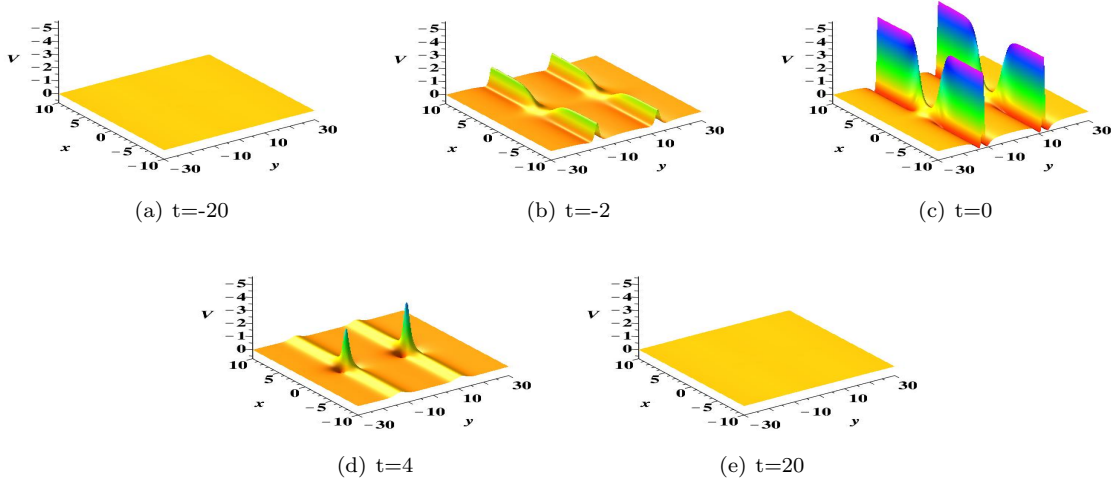


FIGURE 8. The temporal evolution of second-order deformed 2D RW solution  $V^{[2]}$  of equation(1) in the  $(x, y)$ -plane.

the two positive integers  $k$  and  $j$ . We must emphasize that  $\lambda_j$  is a complex constant and  $\lambda_j^* = \lambda_{n+j} = a_n + ib_n$ . When  $a_n > 0$ , the above general  $n$ -th rational-type functions  $U^{[n]}$  and  $V^{[n]}$  are smooth.

**Remark 1** The above solutions  $U^{[n]}$  and  $V^{[n]}$  are rational solutions, if  $\phi(y)$  is a nonzero polynomial function. For example, when  $\phi(y) = 2y$ , the rational solution  $U^{[n]}$  describes the fission of  $n$ -bright lumps and  $n$ -dark lumps from the background plane  $2y$ . The rational solution  $V^{[n]}$  describes the fission of  $2n$ -dark lumps from a constant background plane.

**Remark 2** The above solutions  $U^{[n]}$  and  $V^{[n]}$  are deformed 2D RW solutions, if  $\Phi(y) = \text{sech}(y)$ . The solution  $U^{[n]}$  describes  $2n$  Peregrine-type solitons appear and annihilate from a kink-soliton plan. The solution  $V^{[n]}$  shows that  $n$ -line RWs appear and decay rapidly from a constant background plane, and fission into  $n$  Peregrine-type solitons, and finally disappear in the constant background plane without a trace.

## 5. Summary

In this letter, new bilinear Bäcklund transformation and lax pair of the 2D KdV equation(1) are derived, which are different from the Bäcklund transform and lax pair in Ref.[36, 37]. N-soliton solutions are presented by means of the improved Hirota's bilinear method. Deformed soliton and deformed breather solutions of elastic collision are generated by selecting the appropriate free parameter  $\phi(y)$  see Fig.1 and Fig.2. When  $\Phi(y)$  is a non-constant polynomial function, a family of new rational solutions of the 2D KdV equation are generated using the long wave limit. When  $\Phi(y)$  is a non-zero constant, the rational solutions  $U^{[n]}$  and  $V^{[n]}$  reduce to the rational solution of 2D KdV equation in Ref.[47]. When  $\Phi(y) = \text{sech}(y)$ , the deformed 2D RW solution  $U$  describes a family of Peregrine-type solitons appear and annihilate from a kink-soliton plan. In order to better observe the evolution of the deformed 2D RW solutions, we remove the background plane of  $U$  when plotting see Figs.5 and 7. The deformed 2D RW solution  $V$  shows that a series of line RWs appear and decay rapidly from a constant background plane, and fission into Peregrine-type solitons, and finally annihilate in the constant background plane without a trace see Figs.6 and 8. This paper successfully constructed the deformed 2D RW solutions, which are closely related to the introduced arbitrary function  $\Phi(y)$ . These novel phenomena have never been reported before in nonlinear systems. Our presented work not only provides a new reference method for seeking new exact solutions of nonlinear partial differential equations, but also may be helpful to promote a deeper understanding of nonlinear phenomena.

## Acknowledgments

This work is supported by the NSF of China under Grants No.11671219, No.11871446, No.12071304 and No.12071451.

## References

- [1] Akhmediev N, Ankiewicz A and Taki M 2009 Phys. Lett. A **373** 675-678
- [2] Peregrine D H 1983 J. Aust. Math. Soc. B **25** 16-43
- [3] Guo L J, Wang L H, Cheng Y and He J S 2017 Commun. Nonlinear Sci. Numer. Simulat. **52** 11-23
- [4] Zhang Y S, Guo L J, Chabchoub A and He J S 2017 Rom. J. Phys. **62** 102
- [5] Zhang G Q and Yan Z Y 2018 Commun. Nonlinear Sci. Numer. Simulat. **62** 117-133
- [6] He J S, Xu S W and Porsezian K 2012 Phys. Rev. E **86** 066603
- [7] Li R M, Geng X G and Xue B 2020 J. Nonlinear Math. Phys. **27** 279-294
- [8] Yang J and Zhu Z N 2018 chaos **28** 093103
- [9] Ling L M, Feng B F and Zhu Z N 2016 Physica D **327** 13-29
- [10] Cao Y L, He J S, Cheng Y and Mihalache D 2020 Nonlinear Dyn. **99** 3013-3028
- [11] Gai L T, Ma W X and Li M C 2020 Phys. Lett. A **384** 126178
- [12] Rao J G, Zhang Y S, Fokas A S and He J S 2018 Nonlinearity **31** 4090-4107
- [13] Liu W H, Zhang Y F and Shi D D 2019 Phys. Lett. A **383** 97-102
- [14] Rao J G, Wang L H, Liu W and He J S 2017 Theor. Math. Phys. **193** 1783-1800
- [15] Cao Y L, Malomed B A and He J S 2018 Chaos Soliton and Fract. **114** 99-107
- [16] Ohta Y and Yang J K 2013 J. Phys. A: Math. Theor. **46** 105202
- [17] Rao J G, Mihalache D, Cheng Y and He J S 2019 Phys. Lett. A **383** 1138-1142
- [18] Zhang Y S, Rao J G, Porsezian K and He J S 2019 Nonlinear Dyn. **95** 1133-1146
- [19] Elawady E and Moslem W M 2011 Phys. Plasmas **18** 082306
- [20] Bailung H, Sharma S K and Nakamura Y 2011 Phys. Rev. Lett. **107** 255005
- [21] Bludov Y V, Konotop V V and Akhmediev N 2009 Phys. Rev. A **80** 2962-2964
- [22] Bludov Y V, Konotop V V and Akhmediev N 2010 Eur. Phys. J. Spec. Top. **185** 169-180
- [23] Stenflo L and Marklund M 2010 J. Plasma Phys. **76** 293-295
- [24] Montina A, Bortolozzo U, Residori S and Arecchi F T 2009 Phys. Rev. Lett. **103** 173901
- [25] Solli D R, Ropers C, Koonath P and Jalali B 2007 Nature(London) **450** 1054-1057
- [26] Mihalache D 2017 Rom. Rep. Phys. **69** 403
- [27] Ganshin A N, Efimov V B, Kolmakov G V, Mezhov-Deglin L P and McClintock P V E 2008 Phys. Rev. Lett. **101** 065303
- [28] Guo L J, He J S, Wang L H, Cheng Y, Frantzeskakis D J, Bremer T S and Kevrekidis P G 2020 Physical Review Research **2** 033376
- [29] Boiti M, Leon J J P, Manna M and Pempinelli F 1986 Inverse Probl. **2** 271
- [30] Lou S Y and Hu X B 1997 J. Math. Phys. **38** 6401-6427
- [31] Estevez P G and Leble S 1995 Inverse Probl. **11** 925
- [32] Leble S B and Ustinov N V 1991 Inverse Probl. **10** 617
- [33] Hirota R and Satsma J 1994 J. Phys. Soc. Jpn. **40** 611
- [34] Ablowitz M J and Clarkson P A 1991 Solitons, Nonlinear Evolution Equations and Inverse Scattering (Cambridge: Cambridge University Press)
- [35] Delisle L and Mosaddeghi M 2013 J. Phys. A: Math. Theor. **46** 115203
- [36] Lue X, Tian B, Sun K and Wang P 2010 J. Math. Phys. **51** 113506
- [37] Luo L 2011 Phys. Lett. A **375** 1059-1063
- [38] Wang C J 2017 Nonlinear Dyn. **87** 2635-2642
- [39] Clarkson P A and Mansfield E L 1994 Nonlinearity **7** 795

- [40] Tian B and Gao Y T 1996 Chaos Soliton Fract. **7** 1497-1499
- [41] Lou S Y 1995 J. Phys. A: Math. Theor. **28** 7227-7232
- [42] Hu H C, Tang X Y, Lou S Y and Liu Q P 2004 Chaos Soliton Fract. **22** 327
- [43] Chen Y, Wang Q and Li B 2004 Commun. Theor. Phys. **42** 655-660.
- [44] Fan E G 2009 J. Phys. A **42** 095206
- [45] Luo L 2010 Commun. Theor. Phys. **54** 208-214
- [46] Chen Y R, Song M and Liu Z R 2015 Nonlinear Dyn. **82** 333-347
- [47] Liu Y Q and Wen X Y 2019 Adv. Diff. Equa. **2019** 332
- [48] Wang C J 2016 Nonlinear Dyn. **84** 697-702
- [49] Gilson C, Lambert F, Nimmo J and Willox R 1996 Proc. Roy. Soc. Lond. A **452** 223
- [50] Bell E T 1935 Ann. Math. **35** 258-277
- [51] Fan E G 2011 Phys. Lett. A **375** 493-497
- [52] Luo L 2019 Appl. Math. Lett. **94** 94-98
- [53] Lambert F and Springael J 2001 Chaos Soliton Fract. **12** 2821
- [54] Hirota R 2004 The direct method in soliton theory (Cambridge: Cambridge University Press)
- [55] Ablowitz M J and Satsuma J 1979 J. Math. Phys. **20** 1496-1503

Yulei Cao<sup>1</sup>

<sup>1</sup> Institute for Advanced Study, Shenzhen University, Shenzhen, Guangdong 518060, P. R. China

e-mail: caoyulei@mail.ustc.edu.cn

Peng-Yan Hu<sup>2\*</sup>

<sup>2\*</sup> College of Mathematics and Statistics, Shenzhen University, Shenzhen 518060, China

e-mail: pyhu@szu.edu.cn

Yi Cheng<sup>3</sup>

<sup>3</sup> School of Mathematical Sciences, USTC, Hefei, Anhui 230026, P. R. China

e-mail: chengyi@ustc.edu.cn

Jingsong He<sup>1</sup>

<sup>1</sup> Institute for Advanced Study, Shenzhen University, Shenzhen, Guangdong 518060, P. R. China

e-mail: hejingsong@nbu.edu.cn; jshe@ustc.edu.cn